2023 62nd IEEE Conference on Decision and Control (CDC)
December 13-15, 2023. Marina Bay Sands, Singapore

DISTRIBUTED MODEL PREDICTIVE CONTROLLER FOR THERMAL ENERGY MANAGEMENT SYSTEM OF BATTERY ELECTRIC VEHICLES

Prashant Lokur[1,2], Nikolce Murgovski[1], and Kristian Nicklasson[2]

Abstract— **This paper proposes a distributed model predictive controller (DMPC) that utilizes the alternating direction method of multipliers for the thermal energy management system of a battery electric vehicle. The system comprises a heating, ventilation, and air conditioning unit along with a heat pump. Comparison of the optimal results from a centralized model predictive controller (MPC) and DMPC with those obtained through a rule-based strategy indicate that both the centralized MPC and DMPC deliver energy savings of 9.85 % and 2.21 %, respectively.**

I. INTRODUCTION

The road transport industry plays a significant role in achieving the goal of net zero CO_2 emissions by 2050, given that it currently contributes 16 % of global emissions [1]. One of the primary solutions to reduce emissions is through the use of zero-emission vehicles (ZEVs). Several countries have already taken measures to facilitate the deployment of ZEVs. For example, the United States has set a target of 50 % of light-duty vehicle (LDV) sales being electric vehicles by 2030, while Canada aims to achieve 100 % ZEV LDV sales by 2035. The European Union has mandated that all new cars and vans sold from 2035 to be ZEVs [1]. Among ZEVs, battery electric vehicles (BEVs) are considered the future of passenger vehicles.

A long driving range is a highly desirable feature for prospective buyers of BEVs. However, the limited driving range, which can lead to range anxiety, is a significant concern for non-BEV owners considering a purchase [2]. Although fitting a larger battery may seem like an attractive solution to this issue, it is not a practical option. Doing so would significantly raise the cost, potentially making BEVs less cost-competitive when compared to conventional vehicles. A more cost-effective approach to increasing the driving range is to enhance the system efficiency, which is directly related to reducing energy consumption.

After traction energy, thermal energy management (TEM) system is the second most significant energy consumer in BEVs. The main goal of the TEM system is to meet the thermal demands of the passenger cabin, battery, and electric drive (ED). The TEM's energy consumption becomes prominent in harsh weather conditions, which may result in reducing the electric range by 30-35 % [3]. In addition to decreasing driving range, high energy consumption can also increase the number of charging and discharging cycles of the battery, also known as cycle aging. Thus, high system efficiency can also reduce battery degradation and prolong the battery's life during operation.

Several studies have investigated ways to reduce thermal energy consumption in BEVs, mostly focusing on component-level improvements for the battery thermal management system (BTMS) [4–6] and the heating, ventilation, and air conditioning (HVAC) system [7–13]. While some studies have examined integrated systems, such as [14, 15], they do not reflect the current setup of modern BEVs, which incorporates the HVAC and a heat pump into the TEM system. The system is designed to allow thermal energy transfer between the cabin, battery, and electric drivetrain, which enables the utilization of heat losses from the battery and electric drivetrain. Studies have shown that this setup can be more energy efficient than the conventional system [16–19]. The Tesla Model Y, Polestar 2, and Volvo XC 40, among other modern BEVs, are equipped with a similar TEM system that utilizes an HVAC with a heat pump.

Optimization methods have shown promising results in reducing energy consumption in BEVs. In [6] Pontryagin's maximum principle is investigated to optimize the BTMS. Model Predictive Control (MPC) has emerged as a promising method for energy-optimized control of automotive air conditioning systems [7, 8, 11, 14, 15, 20]. However, in [7, 8, 11, 15, 20], the MPC method is only utilized for the HVAC system rather than for a complete thermal system. One of the challenges in using MPC to control the complete TEM system is the computational demand that arises due to complexity and nonlinearities in the TEM system, making it difficult to operate in real-time in automotive control units.

To reduce computational demand, the authors in [14] propose a decentralized MPC approach for solving the BTMS and HVAC system in a hierarchical manner. However, the results showed that this approach led to a cabin temperature that was 1.5 °C higher than the centralized solution and the battery cooling rate was slow. Additionally, the study steered the battery temperature towards a reference temperature that is not necessarily the optimal battery temperature that minimizes energy consumption subject to temperature limits.

To address the above mentioned shortcomings, this article pioneers the integration of a distributed model predictive controller (DMPC) into the novel TEM system that comprises the battery and HVAC with a heat pump system. The proposed approach utilizes a DMPC that employs the alternating

[1]Prashant Lokur and Nikolce Murgovski are with the Department of Electrical Engineering, Chalmers University of Technology, 412 96 Göteborg, Sweden (e-mail: lokur@chalmers.se, nikolce.murgovski@chalmers.se).

[2]Prashant Lokur and Kristian Nicklasson are with the Department of Thermal Energy Management, China Euro Vehicle Technology AB, 417 55 Göteborg, Sweden (e-mail: prashant.lokur@cevt.se, kristian.nicklasson@cevt.se).

*This work was partially supported by the Energimyndigheten, Sweden under the project number 51459-1

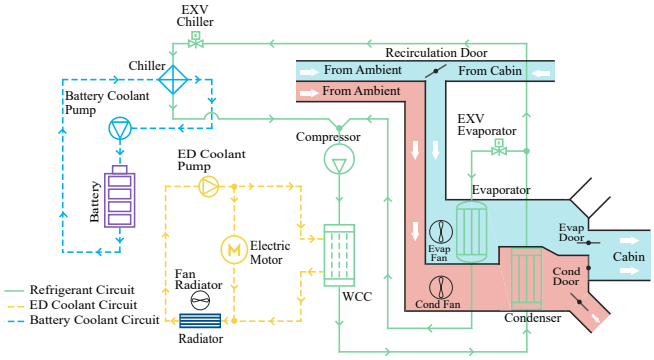

Fig. 1. An architectural overview of the CEVT thermal energy management system (CTEM). The CTEM comprises three circuits: battery coolant (blue circuit), electric drive coolant (yellow circuit), and refrigeration coolant (green circuit). EXV refers to the electronic expansion valve, WCC stands for water cooled condenser and Evap and Cond denote evaporator and condenser, respectively.

direction multipliers method (ADMM) to solve the DMPC problem separately for each subsystem (battery and HVAC) with local information about the other subsystem in order to find optimal operating points for the system for a given scenario. The HVAC subsystem's objective is to minimize the energy consumption of its actuators and track the deviation between the cabin air temperature and the comfortable temperature for passengers. The battery subsystem's objective is to minimize its actuator's energy consumption and regulate battery temperature. This implementation method simplifies the process of addressing nonlinear problems by facilitating parallel computations across different electronic controller units within the vehicle, enhancing its suitability for real-time implementation and potentially reducing computation time.

We apply the optimal controller to a novel architecture developed by the China Euro Vehicle Technology AB, which has some unique features compared to commonly used HVAC and heat pump systems. In particular, the refrigerant loop of the novel system has the potential to be more energy efficient due to the ability to operate in an exhaust heat pump mode [21] – a feature that, e.g., Tesla vehicles do not yet possess.

The paper is organized as follows: Section II introduces the modelling and problem formulation. In Section III, decomposition of the coupled system and ADMM algorithm is presented. Results from solving the problem in a distributed and centralized manner are discussed in Section IV. Finally, Section V draws conclusions from the study and discusses future work.

II. Modelling and Problem Formulation

China Euro Vehicle Technology AB has developed a novel architecture for a battery electric vehicle thermal energy management system (CTEM), as illustrated in Fig. 1. The CTEM system is comprised of three circuits: a battery coolant circuit, an electric drive (ED) coolant circuit, and a refrigeration circuit. The battery coolant circuit includes a battery pump, a cooling plate located beneath the battery pack, and a chiller that transfers heat energy between the coolant and refrigerant circuit. The refrigerant circuit comprises a compressor, a water-cooled condenser, an air condenser, an evaporator, and two expansion valves. The ED coolant circuit consists of a radiator, an electric motor, and an ED coolant pump. Additionally, the CTEM system is equipped with two 4-way valves, enabling thermal energy exchange between different circuits.

This study focuses on a harsh cool-down scenario where the ambient temperature exceeds 45 °C. In this scenario, the battery and cabin are actively cooled using the chiller and the evaporator, respectively, while the ED is passively cooled with the assistance of the radiator. The position of the valves are fixed for the entire drive cycle. The ED circuit is not considered in the study, and the ED coolant temperature and flow rate at the water-cooled condenser inlet are assumed to be at a steady-state. The optimization technique presented in this study utilizes the nonlinear continuous model for the CTEM system in this configuration, which was derived in [21].

The CTEM system in the studied configuration consists of two dynamically coupled subsystems: the battery subsystem and the HVAC subsystem. The cooling rate of the battery is influenced by the coolant temperature at the outlet of the chiller, which is determined by the refrigerant temperature at the inlet of the chiller. Additionally, the refrigerant temperature at the compressor inlet depends on the amount of thermal energy absorbed by the refrigerant from the coolant in the chiller, which is determined by the battery temperature.

A. Battery and HVAC subsystems

The nonlinear dynamics of the battery subsystem are expressed as

$$\dot{x}_{\mathrm{b}} = f_{\mathrm{b}}\left(x_{\mathrm{b}}, u_{\mathrm{b}}, x_{\mathrm{c_s}}, u_{\mathrm{c}}, d\right), \tag{1a}$$

$$x_{\mathrm{b}} = \begin{bmatrix}\mathrm{SOC} & T_{\mathrm{b}}\end{bmatrix}^{\top},\ u_{\mathrm{b}} = \begin{bmatrix}W_{\mathrm{cl}}\end{bmatrix}, \tag{1b}$$

where x_{b} is the battery state vector consisting of the battery state of charge SOC and the battery temperature T_{b}, u_{b} is the control vector consisting of coolant mass flow rate W_{cl}, $x_{\mathrm{c_s}}$ is the subset of HVAC subsystem state vector consisting of refrigerant temperature $T_{\mathrm{c_{in}}}$ and pressure $p_{\mathrm{c_{in}}}$ at the compressor inlet, u_{c} is the HVAC subsystem control input vector and d is the deterministic disturbance that includes traction power demand. The battery subsystem also includes the compressor and heat exchanger models from the HVAC subsystem. The battery subsystem utilizes information from $x_{\mathrm{c_s}}$ and u_{c} to compute the refrigerant inlet temperature at the chiller.

Notice that variables' dependency on time t and planning along the horizon $\tau \in [0, T]$ is omitted in the notation for the sake of simplicity, except later in (9), when the entire problem is summarized. Additionally, in the remainder of the paper, constants are represented with an underline for ease of identification.

The nonlinear dynamics of the HVAC subsystem are expressed as

$$\dot{x}_{\mathrm{c}} = f_{\mathrm{c}}\left(x_{\mathrm{c}}, u_{\mathrm{c}}, x_{\mathrm{b_s}}, u_{\mathrm{b}}\right), \tag{2a}$$

$$x_{\mathrm{c}} = \begin{bmatrix} T_{\mathrm{ca}} & T_{\mathrm{srf}} & T_{\mathrm{m}} & T_{\mathrm{c_{in}}} & p_{\mathrm{c_{in}}} \end{bmatrix}^{\top}, \tag{2b}$$

$$u_{\mathrm{c}} = \begin{bmatrix} \Delta p_{\mathrm{e}} & W_{\mathrm{c}} & W_{\mathrm{ac}} & W_{\mathrm{ae}} & W_{\mathrm{rc}} \end{bmatrix}^{\top}, \tag{2c}$$

where x_{c} is the HVAC state vector consisting of cabin air temperature T_{ca}, cabin interior surface temperature T_{srf}, cabin interior mass temperature T_{m}, refrigerant temperature $T_{\mathrm{c_{in}}}$ and pressure $p_{\mathrm{c_{in}}}$ at the compressor inlet, u_{c} is the HVAC control vector consisting of pressure drop across the expansion valve Δp_{e}, refrigerant mass flow rate at the compressor W_{c}, air mass flow rate at the condenser fan W_{ac}, air mass flow rate at the evaporator fan W_{ae}, W_{rc} refrigerant mass flow rate at the chiller, W_{rc}, and $x_{\mathrm{b_s}} = T_{\mathrm{b}}$ is subset of the battery state vector.

B. Problem formulation

The goal of the TEM system is to minimize energy costs related to the battery and HVAC subsystems. The cost function for the battery subsystem can be expressed as

$$J_{\mathrm{b}}(\cdot) = V_{\mathrm{b}}\left(x_{\mathrm{b}}\right) + \int_{t}^{t+T} \left(P_{\mathrm{bp}}\left(W_{\mathrm{cl}}\right) + \underline{p_{\mathrm{b}}}\delta_{\mathrm{b}}^{2}\right) \mathrm{d}\tau, \tag{3}$$

where $(\cdot)$ is a compact notation for a function of multiple variables, $V_{\mathrm{b}}\big(x_{\mathrm{b}}\big)$ is the terminal cost for the battery subsystem, P_{bp} is the power consumption of the battery coolant pump, δ_b is the slack variable used to soften bounds on the battery temperature, and $\underline{p_{\mathrm{b}}}$ is a coefficient that is tuned to penalize violations of battery temperature bounds,

$$\underline{T_{\mathrm{b_{min}}}} \leq T_{\mathrm{b}} \pm \delta_{\mathrm{b}} \leq \underline{T_{\mathrm{b_{max}}}}, \tag{4}$$

where $T_{\mathrm{b_{min}}}$ and $T_{\mathrm{b_{max}}}$ are minimum and maximum battery temperature, respectively. The relaxation of the temperature bounds is especially important in hot climate conditions when the initial battery temperature could be above the allowed limit.

The cost function for the HVAC subsystem can be expressed as

$$\begin{aligned} J_{\mathrm{c}}(\cdot) =& V_{\mathrm{c}}\left(x_{\mathrm{c}}\right) + \int_{t}^{t+T} \big(P_{\mathrm{comp}}\left(W_{\mathrm{com}}, \Delta p_{\mathrm{com}}\right) + P_{\mathrm{f_{ev}}}\left(W_{\mathrm{ae}}\right) \\ &+ P_{\mathrm{f_{co}}}\left(W_{\mathrm{ac}}\right) + \underline{p_{\mathrm{ca}}}(T_{\mathrm{ca}} - \underline{T_{\mathrm{ca_{ref}}}})^{2})\big)\mathrm{d}\tau, \end{aligned} \tag{5}$$

where P_{comp}, $P_{\mathrm{f_{ev}}}$ and $P_{\mathrm{f_{co}}}$ are the power consumption of the compressor, evaporator fan and condenser fan, respectively, $T_{\mathrm{ca_{ref}}}$ is a reference cabin air temperature, p_{ca} is the penalty on the deviation of the cabin air temperature from the reference, and $V_{\mathrm{c}}\big(x_{\mathrm{c}}\big)$ is the terminal cost for the HVAC subsystem.

The terminal cost for both subsystems is a quadratic function expressed as

$$V_i\big(x_i\big) = \delta x_i^{\top} P_i\, \delta x_i,\ i \in [\mathrm{b}, \mathrm{c}] \tag{6}$$

$$\delta x_i = x_i - x_{i,\mathrm{sp}} \tag{7}$$

where $P_i > 0$ is the solution to the Discrete Algebraic Riccati Equation (DARE) [22] obtained by linearizing the nonlinear subsystems around setpoints, such as $x_{i,\mathrm{sp}}$.

The two coupled subsystems can be equivalently written in the centralized form

$$\dot{x} = F(x, u, d), \tag{8}$$

$$F = \begin{bmatrix} f_{\mathrm{b}}^{\top} & f_{\mathrm{c}}^{\top} \end{bmatrix}^{\top},\ x = \begin{bmatrix} x_{\mathrm{b}}^{\top} & x_{\mathrm{c}}^{\top} \end{bmatrix}^{\top},\ u = \begin{bmatrix} u_{\mathrm{b}}^{\top} & u_{\mathrm{c}}^{\top} \end{bmatrix}^{\top}.$$

The optimization problem can now be formulated as

$$\min_{u, \delta_{\mathrm{b}}} V(x(T)) + \int_{0}^{T} J\left(x(\tau), u(\tau)\right) d\tau \tag{9a}$$

$$\text{s.t. } \dot{x} = F\left(x, u, d\right),\ x(0) = x_0 \tag{9b}$$

$$x \in [x_{\min}, x_{\max}], \tag{9c}$$

$$u \in [u_{\min}, u_{\max}], \tag{9d}$$

$$g\big(x, u\big) \leq 0, \tag{9e}$$

where

$$V = \sum_{i \in [b,c]} V_i(x_i),\ J(x, u) = \sum_{i \in [b,c]} J_i(x_i, u_i),$$

x_0 is the initial state and $g(x, u)$ represents all inequality constraints that ensure safe operation of the CTEM system. The states and control inputs are subjected to upper and lower bounds as expressed in (9c) and (9d).

III. Distributed MPC

It can be noticed that the cost function (9a) of the CTEM system is separable, but coupling between the two subsystems exist in the dynamics (9b) and general inequality constraints (9e). The aim of this section is to decouple the subsystems and then solve the CTEM system in a distributed manner, using ADMM.

A. Decomposition into subsystems

One way to separate the coupled dynamics of the two subsystems is by incorporating a vector of local copies of the coupling state and control variables in each subsystem [23]. Let

$$l_{\mathrm{b}} = \begin{bmatrix} l_{\mathrm{T}} & l_{\mathrm{p}} & l_{\Delta \mathrm{p}} & l_{\mathrm{w_c}} & l_{\mathrm{w_{ac}}} & l_{\mathrm{w_{ae}}} & l_{\mathrm{w_{rc}}} \end{bmatrix}^{\top}, \tag{10}$$

$$l_{\mathrm{c}} = \begin{bmatrix} l_{\mathrm{bT}} & l_{\mathrm{w_{cl}}} \end{bmatrix}^{\top}, \tag{11}$$

denote the local copies in the battery and HVAC subsystem, respectively. Here, l_{T}, l_{p}, $l_{\Delta \mathrm{p}}$, $l_{\mathrm{w_c}}$, $l_{\mathrm{w_{ac}}}$, $l_{\mathrm{w_{re}}}$ are the local copies of $T_{\mathrm{c_{in}}}$, $p_{\mathrm{c_{in}}}$, Δp_{exv}, W_{c}, W_{ac}, W_{ae} and W_{rc} respectively, while l_{bT} and $l_{\mathrm{w_{cl}}}$ are the local copies of T_{b} and W_{cl}, respectively. The battery subsystem is coupled with the $T_{\mathrm{c_{in}}}$ and $p_{\mathrm{c_{in}}}$ states and Δp_{exv}, W_{c}, W_{ac}, W_{ae} and W_{rc} control inputs from the HVAC subsystem, so l_{b} consists of local copies of these variables. Similarly, the local copy l_{c} for the HVAC subsystem consists of local copy of the battery temperature T_{b} and W_{cl}. Then, the dynamics of the battery (1a) and HVAC (2a) subsystems can be rewritten as

$$\dot{x}_{\mathrm{b}} = f_{\mathrm{b}}\left(x_{\mathrm{b}}, u_{\mathrm{b}}, l_{\mathrm{b}}, d\right), \tag{12a}$$

$$\dot{x}_{\mathrm{c}} = f_{\mathrm{c}}\left(x_{\mathrm{c}}, u_{\mathrm{c}}, l_{\mathrm{c}}\right). \tag{12b}$$

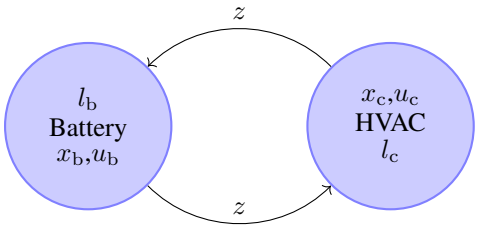

Fig. 2. Illustration of the interdependent subsystems of the CTEM system, with local copies denoted as l_b and l_c utilized to decouple the coupled subsystems. The coordination variable z is employed to bring the local copies into consensus with the true values of each subsystem.

and inequality constraints (9e) can be rewritten as $g_\mathrm{b}(x_\mathrm{b}, u_\mathrm{b}, l_\mathrm{b}) \leq 0$ and $g_\mathrm{c}(x_\mathrm{c}, u_\mathrm{c}, l_\mathrm{c}) \leq 0$.

As the two subsystems now include only copies of the true variables of the other subsystem, a form of negation between the subsystems is needed until consensus is reached on a common value of the local variables [24]. The negotiation is here achieved by introducing coordination variables for each of the local copies

$$z = \begin{bmatrix} z_{\mathrm{bT}} & z_{\mathrm{w_{cl}}} & z_{\mathrm{T}} & z_{\mathrm{p}} & z_{\Delta\mathrm{p}} & z_{\mathrm{w_c}} & z_{\mathrm{w_{ac}}} & z_{\mathrm{w_{ae}}} & z_{\mathrm{rc}} \end{bmatrix}^\top$$

and imposing consistency constraints

$$\begin{aligned} &z_{\mathrm{bT}} = T_\mathrm{b},\ z_{\mathrm{T}} = T_{\mathrm{c_{in}}},\ z_{\mathrm{p}} = p_{\mathrm{c_{in}}},\ z_{\Delta\mathrm{p}} = \Delta p_\mathrm{e},\ z_{\mathrm{w_{ae}}} = w_{\mathrm{ae}} \\ &z_{\mathrm{w_c}} = W_\mathrm{c},\ z_{\mathrm{w_{ac}}} = W_{\mathrm{ac}},\ z_{\mathrm{rc}} = W_{\mathrm{rc}},\ z_{\mathrm{w_{cl}}} = W_{\mathrm{cl}}, \end{aligned} \tag{13a}$$

$$\begin{aligned} &z_{\mathrm{bT}} = l_{\mathrm{bT}},\ z_{\mathrm{T}} = l_{\mathrm{T}},\ z_{\mathrm{p}} = l_{\mathrm{p}},\ z_{\Delta\mathrm{p}} = l_{\Delta\mathrm{p}},\ z_{\mathrm{w_c}} = l_{\mathrm{w_c}}, \\ &z_{\mathrm{w_{ac}}} = l_{\mathrm{w_{ac}}},\ z_{\mathrm{rc}} = l_{\mathrm{w_{rc}}}\ z_{\mathrm{w_{cl}}} = W_{\mathrm{cl}},\ z_{\mathrm{w_{ae}}} = l_{\mathrm{w_{ae}}}. \end{aligned} \tag{13b}$$

The overview of the coupled subsystems, including local copies of variables and coordination variables shared between the two subsystems, is illustrated in Fig. 2.

B. ADMM algorithm

The ADMM algorithm can be now be applied in a general setting. It is configured to minimize an augmented Lagrangian for (9),

$$\begin{aligned} L_\rho(\cdot) = J_\mathrm{b}(\cdot) + J_\mathrm{c}(\cdot) + \sum_{i=1}^{9} \int_0^T \big(&\lambda_\mathrm{z}(i)^\top \left(z(i) - w_\mathrm{z}(i)\right) \\ &+ \frac{\rho}{2} \left(z(i) - w_\mathrm{z}(i)\right)^2 + \lambda_\mathrm{l}(i)^\top \left(z(i) - l(i)\right) \\ &+ \frac{\rho}{2} \left(z(i) - l(i)\right)^2 \big) \mathrm{d}\tau, \end{aligned} \tag{14}$$

where the consistency constraints (13a) and (13b) are adjoined to the cost function (14) by the means of dual variables vectors λ_z and λ_l associated to the each consistency constraint. In addition, the consistency constraints are penalized using penalty parameters $\rho > 0$. Here, $w_\mathrm{z} = \begin{bmatrix} T_\mathrm{b} & W_\mathrm{cl} & T_{\mathrm{c_{in}}} & p_{\mathrm{c_{in}}} & \Delta p_\mathrm{e} & W_\mathrm{c} & W_\mathrm{ac} & W_\mathrm{ae} & W_\mathrm{rc} \end{bmatrix}^\top$, are stacked state and control variables involved in the consistency constraints (13a) and $l = \begin{bmatrix} l_\mathrm{c}^\top & l_\mathrm{b}^\top \end{bmatrix}^\top$, are stacked local copies of both subsystems involved in the consistency constraints (13b).

The augmented Lagrangian (14) can be assigned as the cost function to each subsystem individually. The optimization subproblem for the battery subsystem can be formulated as

$$\min_{u_\mathrm{b}, l_\mathrm{b}, \delta_\mathrm{b}} \ L_\rho\left(x_\mathrm{b}, u_\mathrm{b}, l_\mathrm{b}, z, \lambda_\mathrm{z}, \lambda_\mathrm{l}\right) \tag{15a}$$

$$\text{s.t. } \dot{x}_\mathrm{b} = f_\mathrm{b}\left(x_\mathrm{b}, u_\mathrm{b}, l_\mathrm{b}, u_\mathrm{c}, d\right),\ x_\mathrm{b}(0) = x_{\mathrm{b}_0} \tag{15b}$$

$$x_\mathrm{b} \in [x_{\mathrm{b_{min}}}, x_{\mathrm{b_{max}}}], \tag{15c}$$

$$u_\mathrm{b} \in [u_{\mathrm{b_{min}}}, u_{\mathrm{b_{max}}}], \tag{15d}$$

$$g_\mathrm{b}\left(x_\mathrm{b}, u_\mathrm{b}, l_\mathrm{b}\right) \leq 0, \tag{15e}$$

where $g_\mathrm{b}(\cdot)$ are the general inequality constraints associated with the battery subsystem.

Similarly for the HVAC subsystem the optimization subproblem can be formulated as

$$\min_{u_\mathrm{c}, l_\mathrm{c}} \ L_\rho\left(x_\mathrm{c}, u_\mathrm{c}, l_\mathrm{c}, z, \lambda_\mathrm{z}, \lambda_\mathrm{l}\right) \tag{16a}$$

$$\text{s.t. } \dot{x}_\mathrm{c} = f_\mathrm{c}\left(x_\mathrm{c}, u_\mathrm{c}, l_\mathrm{c}, u_\mathrm{b}\right),\ x_\mathrm{c}(0) = x_{\mathrm{c}_0} \tag{16b}$$

$$x_\mathrm{c} \in [x_{\mathrm{c_{min}}}, x_{\mathrm{c_{max}}}], \tag{16c}$$

$$u_\mathrm{c} \in [u_{\mathrm{c_{min}}}, u_{\mathrm{c_{max}}}], \tag{16d}$$

$$g_\mathrm{c}\left(x_\mathrm{c}, u_\mathrm{c}, l_\mathrm{c}\right) \leq 0, \tag{16e}$$

where $g_\mathrm{c}(\cdot)$ are the general inequality constraints associated with the HVAC subsystem.

The optimization subproblems (15) and (16) can now be solved in a distributed manner using the separable augmented Lagrangian (14) [24].

The ADMM iterations consist of a minimization step for the primal variables u_b, u_c and local variables l_b, l_c, a minimization step for the coordination variables z, and an update step for the dual variables λ_z, λ_l. The z coordination variable minimization step can be analytically solved, as z is not involved in the system dynamics (12a), (12b). The z minimization step for k^{th} iteration can be expressed as

$$z^{k+1} = \frac{1}{2}\left(w_\mathrm{z}^{k+1} + l^{k+1} - \frac{1}{\rho}\left(\lambda_\mathrm{z}^k + \lambda_\mathrm{l}^k\right)\right). \tag{17}$$

The convergence of the ADMM algorithm is determined by evaluating the progress of z, λ_z, and λ_l between two iterations, which is a direct measure of the residual of the consistency constraints (13). This is achieved using a stopping criterion based on the norm of the current iteration x_z and a constant $e > 0$ [23]. Selecting the appropriate value of e can help achieving the desired accuracy, however, a lower value of e requires more iterations.

Within the MPC framework, the ADMM algorithm has to be iterated until the stopping criterion is met in each MPC step, as summarized in Algorithm 1. To differentiate the iterations of the MPC update variables from the iteration in ADMM, a superscript h is assigned to MPC iterations, e.g., x^h and u^h, while a superscript k is assigned to ADMM iterations. For the first MPC step, z^0, λ_z^0, and λ_l^0 are initialized with appropriate values. In subsequent MPC steps, the values rely on solutions from the previous step.

Algorithm 1 ADMM for a single MPC step h

Input: $x_{\mathrm{b}_0}^h$, $x_{\mathrm{c}_0}^h$, d^h
Output: u_{b}^h, u_{c}^h

if $h == 0$ **then**
  Initialization: λ_{z}^0, λ_{l}^0, z^0, $\rho > 0$ (penalty term), $e > 0$ (stopping criterion) and M (maximum iterations)
end if
for $k = 1$ to M **do**
  Compute u_{b}^{k+1}, l_{b}^{k+1} and x_{b}^{k+1} by solving (15) utilizing
  λ_z^k, λ_l^k, z^k and $x_{\mathrm{b}_0}^h$.
  Compute u_{c}^{k+1}, l_{c}^{k+1} and x_{c}^{k+1} by solving (16) utilizing
  λ_z^k, λ_l^k, z^k and $x_{\mathrm{c}_0}^h$.
  Compute z^{k+1} using (17) with w_{z}^{k+1}, l^{k+1}, λ_{z}^k and λ_{l}^k.
  Update the dual variables
  $\lambda_{\mathrm{z}}^{k+1} \leftarrow \lambda_{\mathrm{z}}^k + \rho(z^{k+1} - w_{\mathrm{z}}^{k+1})$
  $\lambda_{\mathrm{l}}^{k+1} \leftarrow \lambda_{\mathrm{l}}^k + \rho(z^{k+1} - l^{k+1})$
  if $\left\| \begin{matrix} z^{k+1} - z^k \\ \lambda_{\mathrm{z}}^{k+1} - \lambda_{\mathrm{z}}^k \\ \lambda_{\mathrm{l}}^{k+1} - \lambda_{\mathrm{l}}^k \end{matrix} \right\|_{L^\infty} \leq e \left\| w_{\mathrm{z}}^{k+1} \right\|$ **then**
    $u_{\mathrm{b}}^h \leftarrow u_{\mathrm{b}}^{k+1}$
    $u_{\mathrm{c}}^h \leftarrow u_{\mathrm{c}}^{k+1}$
    break
  end if
end for

IV. Results

This section presents and discusses the results obtained from applying the ADMM-based DMPC method and centralized optimization approaches.

A. Simulation Setup

The simulations were conducted on the Worldwide harmonized Light vehicles Test Cycle (WLTC) with an ambient temperature of 46 °C. The traction power demand was obtained from the WLTC simulation data. The $\underline{T_{\mathrm{ca_{ref}}}}$ was set to 21 °C, and $\underline{T_{\mathrm{b_{min}}}}$ and $\underline{T_{\mathrm{b_{max}}}}$ bounds for the battery temperature were set to 12 °C and 26 °C, respectively.

The centralized optimal control problem (9) and the subproblems (15) and (16) were discretized using the Runge-Kutta 4th order method with a sampling time of 1 s to form NLPs in a standard form. To solve the discretized NLP problems, a direct multiple shooting method was employed with the help of CasADi in MATLAB and the problem was then solved with the Interior Point Optimizer (IPOPT) solver [25]. The NLP problems were executed on a laptop PC equipped with an Intel Core i7 processor operating at 2.6 GHz and 32 GB RAM.

B. Optimal results

We analyze the optimal solution of the centralized and distributed MPC by comparing with a rule-based strategy that regulates the battery and cabin air temperatures. Fig. 3 illustrates the trajectories of these states obtained by the three strategies. The battery temperature trajectory obtained using DMPC follows a similar trend to the centralized method, but it exhibits a much faster cooling rate. Consequently, the DMPC method reaches the upper bound of the battery temperature earlier than the centralized method. However, due to the minimum coolant flow rate constraint, the battery temperature continues to decrease.

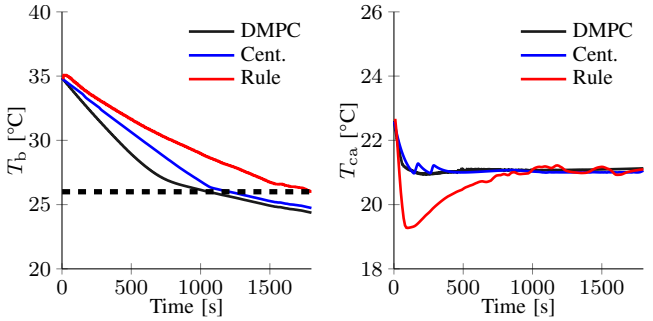

(a) Battery Temperature. The dashed line represents the upper limit.

(b) Cabin Temperature.

Fig. 3. The state trajectories obtained using the centralized and DMPC control strategy on the CTEM. Both solutions are compared with the rule-based strategy.

The cabin air temperature trajectory obtained using DMPC is also similar to the one obtained from the centralized solution, with a maximum deviation of 0.12 °C from the reference temperature. This is well within the acceptable deviation range, which is not surprising, since the cabin temperature regulation appears directly in the cost function and upon convergence DMPC tends to reach the target temperature similarly as the centralized MPC. In addition to maintaining the reference temperature in the cabin, it is also important that the cabin is cooled to the reference temperature as soon as possible. The T_{ca} in DMPC method takes a similar amount of time to reach the reference temperature as in the centralized solution.

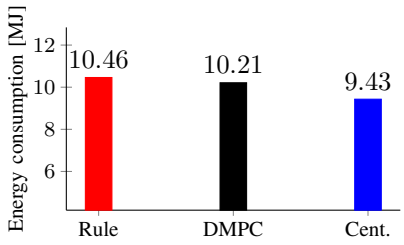

Fig. 4. The energy consumption of the CTEM system is regulated by the three different methods. The energy consumption here includes the energy consumption of the compressor, battery coolant pump, evaporator, and condenser fan.

The centralized and DMPC algorithms resulted in an energy reduction of 9.85 % and 2.21 %, respectively, compared to the rule-based strategy. The energy reduction achieved is mainly due to the higher cooling rate for the battery temperature at the beginning of the drive cycle. This results in a lower energy consumption for the battery and compressor for the rest of the drive cycle. It is important to note that in

the given harsh scenario, the system operates at its limits as it has to cool down both the battery and the cabin, which doesn't provide much freedom for energy reduction.

Most importantly, the DMPC method can offer computational efficiency over the centralized approach by allowing the subsystems to be solved separately. The battery and HVAC subsystems, which have 2 and 5 states respectively, require fewer states than the 7 states in the centralized approach, leading to a reduction in computational effort. This can be advantageous in real-time applications, where fast and efficient solutions are required.

V. Conclusion and future work

This paper presents a DMPC method for optimizing a novel thermal management system for BEVs. By decoupling the battery and HVAC subsystems using dual decomposition and ADMM, the proposed distributed method reduces the computation demand on the electronic controller unit, enabling it to be implemented in real-time. Compared to a rule-based strategy, the results demonstrate that the proposed DMPC method can reduce energy consumption by 2.21 %, which in turn would increase the driving range of BEVs. Moreover, this method is not limited to the studied CTEM system and can directly be applied to other thermal management systems in BEVs.

The extension of the proposed method to include the ED coolant circuit presents an exciting opportunity for future research in this area. Additionally, exploring the impact of the stopping criterion on the convergence of the algorithm will provide further insights into the performance of the proposed method.

References

[1] L. Paoli, A. Dasgupta, and S. McBain, "Electric vehicles," 2022. [Online]. Available: https://www.iea.org/reports/electric-vehicles

[2] D. Pevec, J. Babic, A. Carvalho, Y. Ghiassi-Farrokhfal, W. Ketter, and V. Podobnik, "A survey-based assessment of how existing and potential electric vehicle owners perceive range anxiety," *Journal of cleaner Production*, vol. 276, p. 122779, 2020.

[3] P. E and D. G. M. M. G. M. U. et al., "Experimental test campaign on a battery electric vehicle: On-road test results (part 2)," *SAE Int. J. Alt. Power.*, vol. 4(2), pp. 277–292, 2015.

[4] S. Park and C. Ahn, "Computationally efficient stochastic model predictive controller for battery thermal management of electric vehicle," *IEEE Transactions on Vehicular Technology*, vol. 69, no. 8, pp. 8407–8419, 2020.

[5] J. Lopez-Sanz, C. Ocampo-Martinez, J. Alvarez-Florez, M. Moreno-Eguilaz, R. Ruiz-Mansilla, J. Kalmus, M. Gräeber, and G. Lux, "Nonlinear model predictive control for thermal management in plug-in hybrid electric vehicles," *IEEE Transactions on Vehicular Technology*, vol. 66, no. 5, pp. 3632–3644, 2017.

[6] S. Bauer, A. Suchaneck, and F. Puente León, "Thermal and energy battery management optimization in electric vehicles using pontryagin's maximum principle," *Journal of Power Sources*, vol. 246, pp. 808–818, 2014. [Online]. Available: https://www.sciencedirect.com/science/article/pii/S0378775313013591

[7] S. Schaut and O. Sawodny, "Thermal management for the cabin of a battery electric vehicle considering passengers' comfort," *IEEE Transactions on Control Systems Technology*, vol. 28, no. 4, pp. 1476–1492, 2019.

[8] D. Kibalama, Y. Liu, S. Stockar, and M. Canova, "Model predictive control for automotive climate control systems via value function approximation," *IEEE Control Systems Letters*, vol. 6, pp. 1820–1825, 2022.

[9] Y. Xie, Z. Liu, K. Li, J. Liu, Y. Zhang, D. Dan, C. Wu, P. Wang, and X. Wang, "An improved intelligent model predictive controller for cooling system of electric vehicle," *Applied Thermal Engineering*, vol. 182, p. 116084, 2021. [Online]. Available: https://doi.org/10.1016/j.applthermaleng.2020.116084

[10] M. Alizadeh, S. Dhale, and A. Emadi, "Model predictive control of HVAC system in a battery electric vehicle with fan power adaptation for improved efficiency and online estimation of ambient temperature," in *IECON 2021 – 47th Annual Conference of the IEEE Industrial Electronics Society*, 2021, pp. 1–6.

[11] F. Ju, N. Murgovski, W. Zhuang, and L. Wang, "Integrated propulsion and cabin-cooling management for electric vehicles," *Actuators*, vol. 11, no. 12, 2022. [Online]. Available: https://www.mdpi.com/2076-0825/11/12/356

[12] M. A. Jeffers, L. Chaney, and J. P. Rugh, "Climate control load reduction strategies for electric drive vehicles in cold weather," *SAE International Journal of Passenger Cars-Mechanical Systems*, vol. 9, no. 2016-01-0262, pp. 75–82, 2016.

[13] K. Kambly and T. H. Bradley, "Geographical and temporal differences in electric vehicle range due to cabin conditioning energy consumption," *Journal of Power Sources*, vol. 275, pp. 468–475, 2015. [Online]. Available: https://www.sciencedirect.com/science/article/pii/S0378775314017613

[14] M. R. Amini, H. Wang, X. Gong, D. Liao-McPherson, I. Kolmanovsky, and J. Sun, "Cabin and battery thermal management of connected and automated hevs for improved energy efficiency using hierarchical model predictive control," *IEEE Transactions on Control Systems Technology*, vol. 28, no. 5, pp. 1711–1726, 2019.

[15] H. Wang, Y. Meng, Q. Zhang, M. R. Amini, I. Kolmanovsky, J. Sun, and M. Jennings, "Mpc-based precision cooling strategy (pcs) for efficient thermal management of automotive air conditioning system," in *2019 IEEE Conference on Control Technology and Applications (CCTA)*, 2019, pp. 573–578.

[16] Z. Zhang, D. Wang, C. Zhang, and J. Chen, "Electric vehicle range extension strategies based on improved ac system in cold climate – a review," *International Journal of Refrigeration*, vol. 88, pp. 141–150, 2018. [Online]. Available: https://www.sciencedirect.com/science/article/pii/S0140700718300033

[17] J. J. Meyer, J. Lustbader, N. Agathocleous, A. Vespa, J. Rugh, and G. Titov, "Range extension opportunities while heating a battery electric vehicle," *SAE Technical Paper*, 2018. [Online]. Available: https://doi.org/10.4271/2018-01-0066

[18] T. Kondo, A. Katayama, H. Suetake, and M. Morishita, "Development of automotive air-conditioning systems by heat pump technology," *Mitsubishi Heavy Industries Technical Review*, vol. 48, no. 2, pp. 27–32, 2011.

[19] S. Osborne, J. Kopinsky, S. Norton, A. Sutherland, D. Lancaster, E. Nielsen, A. Isenstadt, and J. German, "Automotive thermal management technology," *Automotive News*, 2015.

[20] Y. Huang, A. Khajepour, F. Bagheri, and M. Bahrami, "Modelling and optimal energy-saving control of automotive air-conditioning and refrigeration systems," *Proceedings of the Institution of Mechanical Engineers, Part D: Journal of Automobile Engineering*, vol. 231, no. 3, pp. 291–309, 2017.

[21] P. Lokur, K. Nicklasson, L. Verde, M. Larsson, and N. Murgovski, "Modeling of the thermal energy management system for battery electric vehicles," in *2022 IEEE Vehicle Power and Propulsion Conference (VPPC)*, 2022, pp. 1–7.

[22] J. B. Rawlings, D. Q. Mayne, and M. Diehl, *Model predictive control: theory, computation, and design*. Nob Hill Publishing Madison, WI, 2017, vol. 2.

[23] A. Bestler and K. Graichen, "Distributed model predictive control for continuous-time nonlinear systems based on suboptimal ADMM," *Optimal Control Applications and Methods*, vol. 40, pp. 1–23, 2019.

[24] S. Boyd, N. Parikh, E. Chu, B. Peleato, J. Eckstein *et al.*, "Distributed optimization and statistical learning via the alternating direction method of multipliers," *Foundations and Trends® in Machine learning*, vol. 3, no. 1, pp. 1–122, 2011.

[25] J. A. Andersson, J. Gillis, G. Horn, J. B. Rawlings, and M. Diehl, "Casadi: a software framework for nonlinear optimization and optimal control," *Mathematical Programming Computation*, vol. 11, pp. 1–36, 2019.